Transition Between the Massive Reef-Backreef and Cyclic Lagoon Facies of the Dachstein Limestone in the Southern Part of the Dachstein Plateau, Northern Calcareous Alps, Upper Austria and Styria

János Haas[1], Olga Piros[2], Tamás Budai[2], Ágnes Görög[3],
Gerhard W. Mandl[4] & Harald Lobitzer[5]

4 Text-Figures, 6 Plates

Österreichische Karte 1:50.000
Blatt 127 Schladming

Northern Calcareous Alps
Dachstein Limestone
Microfacies
Paleokarst
Triassic
Norian

Contents

Der Dachsteinkalk im Übergangsbereich vom massigen Riff/Rückriff zur zyklisch gebankten „lagunären" Entwicklung am südlichen Dachstein-Plateau, Nördliche Kalkalpen, Oberösterreich

Zusammenfassung

Im südlichen Dachstein-Plateau verzahnt massiger norischer Dachstein-Riffkalk gegen Norden zu mit zyklisch gebanktem „lagunärem" Dachsteinkalk. Dieser Übergangsbereich wird beschrieben und interpretiert. Der zyklisch gebankte Dachsteinkalk wird aus Wechselfolgen von subtidalen mit peritidalen Ablagerungen aufgebaut. Die subtidalen Kalkbänke sind oftmals onkoidisch entwickelt und enthalten Megalodonten, Gastropoden und charakteristische Foraminiferen-Assoziationen. Einige der subtidalen Bänke zeigen pedogenetische und Paläokarst-Phänomene sowie Erscheinungen meteorischer Früh-diagenese. Die peritidalen Bänke sind durch umgelagertes Paläoböden-Material oftmals rot gefärbt und zeigen manchmal beginnende Pedogenese. Aufgrund der Foraminiferen-Assoziationen sowie der geologischen Situation kann der Dachsteinkalk in der Umgebung der Handgruben als obernorisch betrachtet werden. Schließlich werden unsere Profile mit gleichaltrigen zyklischen Ablagerungen der inneren Karbonatplattform des nördlichen Dachstein-Plateaus in der Umgebung des Krippensteins und mit den Dachsteinkalk-Abfolgen des nordöstlichen Transdanubischen Mittelgebirges in Ungarn verglichen, die ähnliche sedimentologische Phänomene sowie paläogeographische Muster aufweisen.

Abstract

Along the southern margin of the Dachstein Group Norian massive reef limestones are exposed that progress northward into well-bedded cyclic peritidal-lagoonal carbonates. Characteristic features of the transitional zone are described and interpreted. The cyclic succession is made up of an alternation of subtidal and peritidal beds. The subtidal beds are usually oncoidal and contain megalodonts, gastropods, and foraminifera. Some of the subtidal beds were affected by pedogenic alteration, karstification and meteoric early diagenesis. The peritidal beds are usually red; they contain reworked soil derived material and were also affected by incipient pedogenesis. Based on the foraminifera fauna and considering also the geological setting, the studied beds at Handgruben can be assigned to the Upper (?) Norian. The studied sections are compared with the coeval cyclic internal platform deposits, which occur in the northern part of the Dachstein Plateau (Krippenstein) and with the Dachstein Limestone successions of the NE part of the Transdanubian Range in Hungary showing similar sedimentological features and paleogeographic setting.

1 János Haas: Geological, Geophysical and Space Science Research Group of the Hungarian Academy of Sciences, Eötvös Loránd University,
   Pázmány sétány 1/C, H 1117 Budapest, Hungary. haas@ludens.elte.hu
2 Olga Piros, Tamás Budai: Hungarian Geological Institute, Stefánia út 14, H 1143 Budapest, Hungary. piros@mafi.hu; budai@mafi.hu
3 Ágnes Görög: Paleontological Department, Eötvös Loránd University, Pázmány sétány 1/C, H 1117 Budapest, Hungary. gorog@ludens.elte.hu
4 Gerhard W. Mandl: Geologische Bundesanstalt, Neulinggasse 38, A 1030 Vienna. Gerhard.Mandl@geologie.ac.at
5 Harald Lobitzer: Lindaustraße 3, A 4820 Bad Ischl, Austria. harald.lobitzer@aon.at

Introduction

The Dachstein Mountain range is the type locality of the Dachstein Limestone and the Dachstein-type carbonate platforms. This area is made up predominantly of the cyclic inner platform facies of the Dachstein Limestone. However, at the southern part of the Dachstein Group massive Norian reef limestones are exposed in a zone a few hundred meters wide (RONIEWICZ et al., 2007), while the transition to the slope, respectively, open-sea facies of the Hallstatt basin is mostly tectonically truncated. Only a few examples of this transition are preserved, e.g. at Gosaukamm (WURM, 1982; KRYSTYN et al., 2009). The aim of the present paper is to display the transition between the two characteristic facies of the Dachstein platform. We tried to figure out how the massive reef facies progresses into the cyclic peritidal-lagoonal one. Determination and characterisation of the building elements of the near-reef but already cyclic successions are also the subject of the present work. A comparative analysis of the studied sections with those previously investigated in the Krippenstein area 5–6 km northward will also be performed. Facies conditions akin to that in the Dachstein Plateau are known in the NE part of the Transdanubian Range, Hungary. Therefore we extended the comparative facies analysis also to this area.

Geological Setting

The Dachstein Group represents a segment of the margin of the Tethys (Neotethys) Ocean and accordingly, stratigraphical and lithofacies characteristics of this area reflect the general evolutionary history of this realm. Permian evaporites are overlain by Lower Triassic shallow marine siliciclastics (Werfen Formation), that are followed by Lower to Middle Anisian shallow marine carbonates (Gutenstein and Steinalm Formations). These formations are exposed at the base of the Dachstein Nappe along the southern, southwestern margin of the Dachstein Plateau (MANDL, 2000) – see also Text-Fig. 1. In the Late Anisian, in connection with the Neotethys opening pelagic basins developed over large areas where grey cherty and variegated limestones were formed. However, in some places the shallow marine conditions prolonged giving rise to the development of Wetterstein-type carbonate platforms; then in the Ladinian to Early Carnian the platforms prograded onto the adjacent basins. The Wetterstein-type platform carbonates are also widely exposed along the southern slopes of the Dachstein Plateau. A sea-level drop in the Early Carnian led to subaerial exposure over a predominant part of the former Wetterstein platform and significant erosion (Text-Fig. 2). As a result of the Late Carnian transgression, the shallow marine-lagoonal conditions resumed in
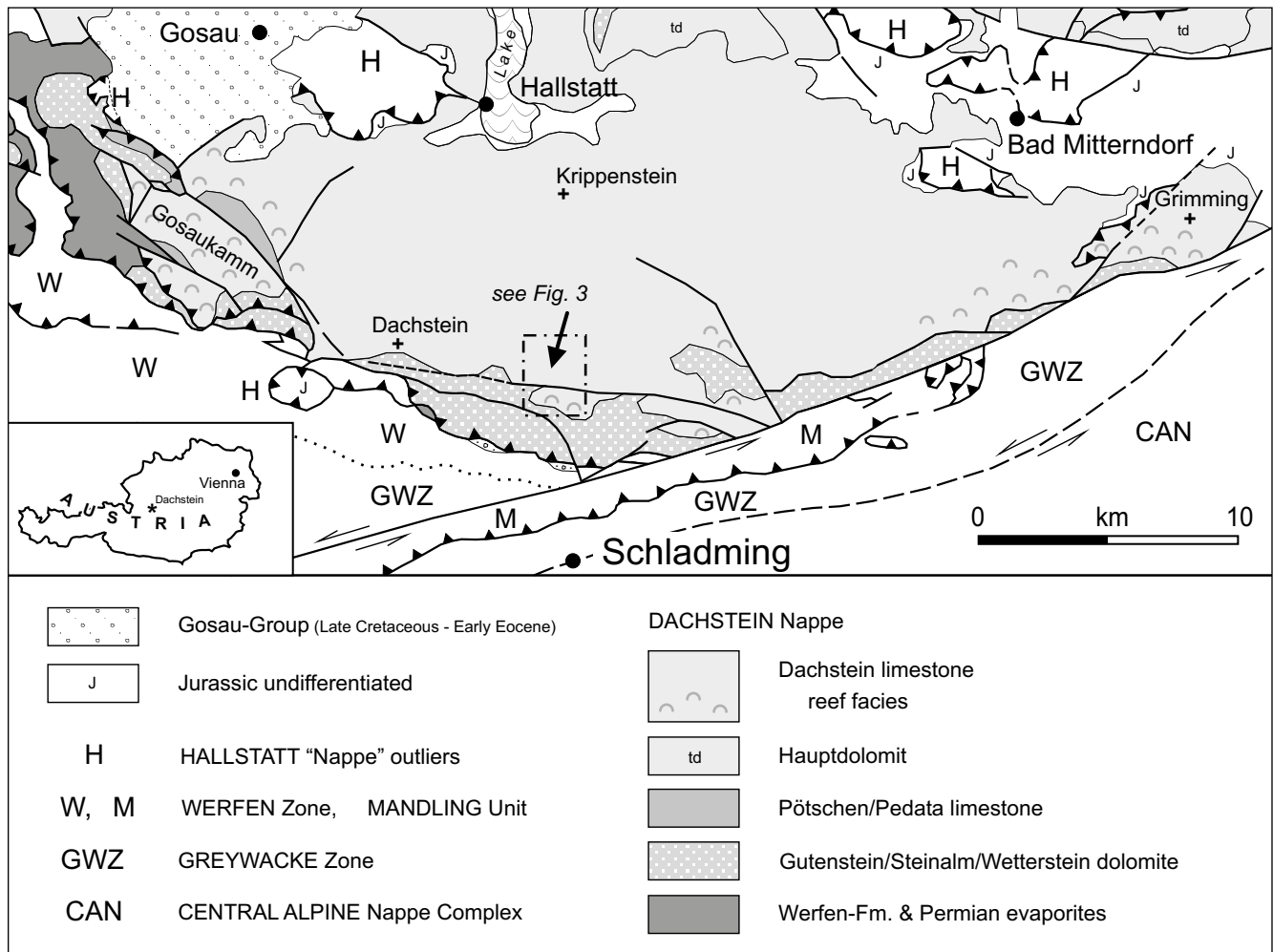
Text-Fig. 1.
Geological sketch of the Dachstein area, displaying the area studied.

the depressions of the erosion affected previous platform (Waxeneck Limestone). The rising sea-level in the latest Tuvalian led to the extension of pelagic conditions, whereas on the local highs shallow marine conditions prevailed and reef-patches developed supplying the adjacent peri-platform basins (RONIEWICZ et al., 2007). This episode was followed by rapid progradation of the Dachstein platform in the early Norian i.e. the onset of the Dachstein platform evolution (Text-Fig. 2). After an episodic transgression, aggradational evolution for the Middle Norian (Alaunian), slow progradation for the Late Norian (Sevatian) and accelerated progradation for the early Rhaetian was interpreted from the Gosaukamm and Gosausee marginal successions, and the Dachstein reef building came to an end by a drowning event in the middle Rhaetian (KRYSTYN et al., 2009).

The area of our study is located between the Guttenberg mountain lodge and locality "Bei der Hand", north to Feisterscharte, in the southern part of the Dachstein Plateau (Text-Figs. 1, 3). According to the geological maps (MANDL & MATURA, 1995; MANDL, 2001), a northward regional dip characterises the southern part of the Dachstein Plateau, although there are several tilted blocks of various dip.

NE to the Guttenberg lodge at the base of the slope of Mt. Sinabell the erosion-formed uneven top of the Wetterstein Dolomite is well visible. Above it reddish dolomites occur from which Carnian conodonts *(Metapolygnatus polygnathiformis)* were encountered (RONIEWICZ et al., 2007). It is overlain by massive carbonates of very inhomogeneous facies composition (Text-Figs. 2, 3). According to facies investigations of RONIEWICZ et al. (2007) the reef-detritus facies are predominant; the proximal backreef facies are also common, whereas the biolithite facies are rare. Intercalations of pelagic facies containing reef-derived components were also encountered (Text-Figs. 2, 3). These beds yielded earliest Norian (Lacian 1) conodonts *Epigondolella primitia* (LEIN, 1987), later on revised by KRYSTYN et al. (2009) as *Epigondolella quadrata*. In a sample taken on the path to Mt. Sinabel and on the NE side of Mt. Eselstein conodonts indicating Lacian 2 were found (RONIEWICZ et al., 2007).

According to RONIEWICZ et al. (2007) north to the inhomogeneous massive carbonates massive backreef facies occurs which extends over the Seetal Fault northward (Text-Figs. 2, 3). It is typified by a) biosparite (rudstone and grainstone) with poorly sorted bioclasts and grapestones and b) biopelmicrite with Rivulariaceans. At the base of this facies poorly preserved Middle Norian conodonts were reported.

Results

The Boundary Between the Massive and the Bedded Dachstein Limestone

From the massive limestones south to the Seetal Fault (Text-Fig. 3) we took only a few samples. Results of our microfacies studies met with observations of RONIEWICZ et al. (2007).

Reef-derived breccias with mm to cm-sized lithoclasts and bioclasts were usually found in the samples studied. Fragments of microbial crust (Plate 1, Fig. 2), micro-encruster microproblematicum *Radiomura cautica*, Rivulariaceans (Plate 1, Fig. 4), corals (Plate 1, Fig. 1), calcareous sponges (Plate 1, Fig. 3) (sphinctozoans and inozoans), crinoids, bivalves,

gastropods, ammonites, ostracods were encountered in most of the samples. Encrusting foraminifera *(Tolypammina gregaria)* are common (Plate 1, Fig. 5). Miliolinids *(Agathammina austroalpina)*, Duostominidae, *Ophthalmidium triadicum*, *Ophthalmidium* sp., *Agathammina* sp., Textulariidae, *Austrocolomia* sp., *Turrispirillina* sp., *Kaevaria fluegeli*, *Miliolipora cuvillieri*, *Orthotrinacria expansa* were also found (Plate 2, Figs. 1–5). There are various lithoclasts (e.g. peloidal micrite, ostracodal micrite, ostracodal sparite, bioclastic micrite, oolitic grainstone).

The near reef or the protected platform was the habitat of the *Agathammina austroalpina* (e.g. ZANINETTI, 1976; BERNECKER, 1996). *Orthotrinacria expansa* is considered as a reefal porcelaneous foraminifer (ZANINETTI & MARTINI, 1993). *Kaevaria fluegeli* was a reef-cavity dweller (e.g. DULLO, 1980; SENOWBARI-DARYAN et al., 1982). Duostominids preferred the outer reef and the calcarenitic substrate; oncoid and grapestone facies (e.g. HOHENEGGER & PILLER, 1975; SCHÄFER & SENOWBARI-DARYAN, 1978; DULLO, 1980; GAŹDZICKI, 1983; BERNECKER, 1996).

According to our observation the boundary between the massive and the cyclic limestones can be recognised at a fault, 400 m north to the Seetal Fault (Text-Fig. 2). However, there is no abrupt change in the structural and textural features of the limestone at the fault. Accordingly the fault does not play a significant role in the determination of the present-day facies distribution.

In a sample taken about 100 m south to the above-mentioned fault (that is 300 m north to the Seetal Fault) a boundstone type facies was recognised, that is characterised by abundance of microbial crusts (Plate 1, Fig. 7), and encrusting larger foraminifera, *Alpinophragmium perforatum* (Plate 1, Fig. 6). A few miliolinids, Textulariidae and microproblematicum *Baccanella floriformis* also occur (Plate 1, Fig. 8). There are a number of solution cavities, some of them after microbially encrusted bioclasts which are filled by sparry calcite. *Alpinophragmium perforatum* is a reefal larger foraminifera species, a typical encruster in the Norian–Rhaetian well-ventilated central reef or forereef environments (FLÜGEL, 1967; HOHENEGGER & LOBITZER, 1971; DULLO, 1980; BERNECKER, 1996; WURM, 1982; SENOWBARI-DARYAN et al., 1982; GAŹDZICKI, 1983).

Another sample was taken just at the fault (marked by D1 on Text-Figs. 2, 3). It has a peloidal microsparite texture with a few bioclasts (fragments of molluscs, foraminifera, *Thaumatoporella*). Duostominidae *(Variostoma* sp., *Diplotremina* sp.) are common; *Trochammina* spp. and microproblematicum *Messopotamella angulata* also occur (Plate 2, Figs. 6, 7). It is abundant in fenestral fabrics. This microfacies is similar to the biopelmicritic sub-facies of the massive backreef facies of RONIEWICZ et al. (2007).

Section Handgruben A

About 100 m north to the boundary between the massive and the bedded Dachstein Limestone, a more than 1 m thick brownish red limestone intercalation was found between grey limestone beds. In this outcrop (marked by H–A on Text-Figs. 2, 3) four beds could be distinguished (Plate 3, Fig. 1).

The lowermost exposed bed (Bed 1) is dasycladalean grainstone; fine to coarse-grained calcarenite (Plate 4, Figs. 1, 2, 3). The origin of the fine bioclast fraction cannot be recognised, probably detritus of calcareous algae
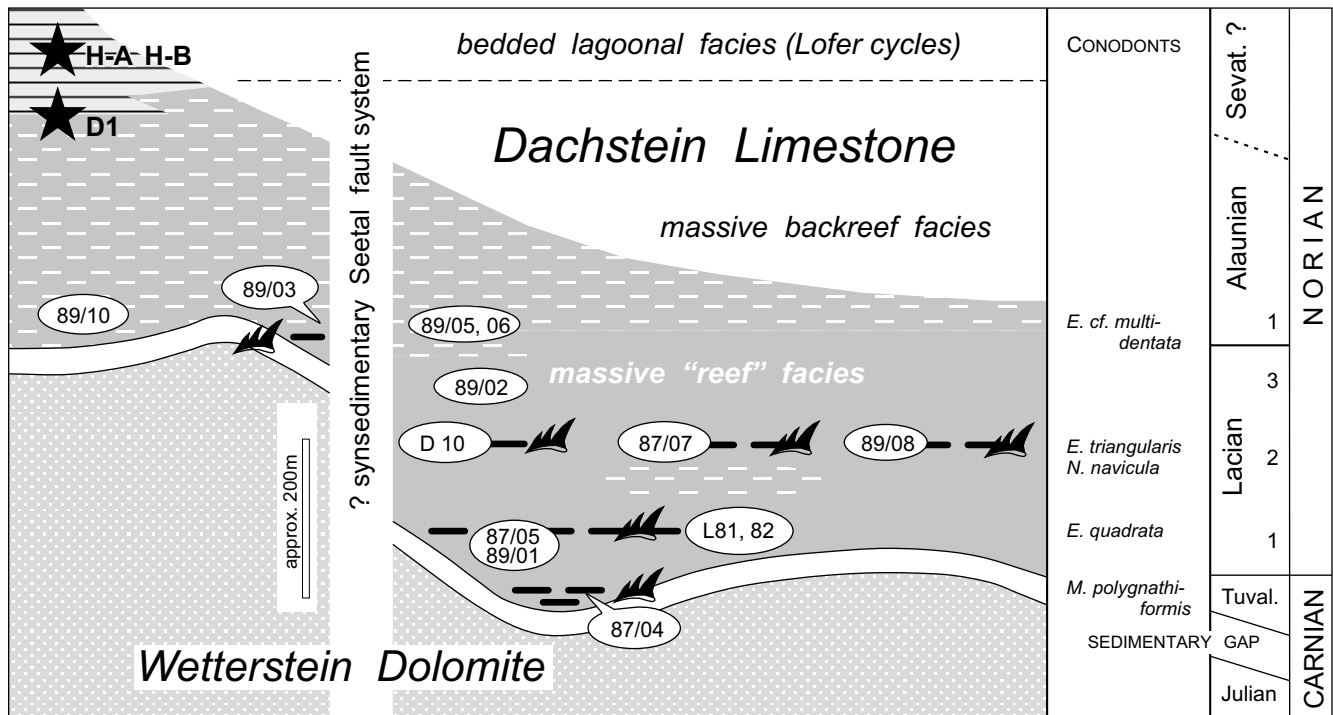
Text-Fig. 2.
Stratigraphic scheme of the Upper Triassic formations for the Feisterscharte area (after RONIEWICZ et al., 2007, modified). Not to scale!

and molluscs. The coarse fraction is made up mostly of dasycladalean algae (1–8 mm in size), foraminifera, and gastropods. Foraminiferans are mostly recrystallised Aulotortidae *(Aulotortus sinuosus, A. impressus, A. friedli, A. communis)* beside them few specimens of *Ophthalmidium* could be recognised (Plate 2, Figs. 8–11). A few embryonic ammonites also occur. There are mm-sized solution vugs with sparitic fill similar to those in the moulds of dasycladaleans and gastropods.

The next bed is 25 cm thick (Bed 2) and dark grey limestone with black clasts. The texture is peloidal, bioclastic wackestone with a pedogenic overprint. There are fragments of molluscs, calcimicrobes, few gastropods and a relatively rich foraminifera fauna. *Turrispirillina minima* and Aulotortidae *(Aulotortus communis, A. impressus, A. tenuis, A. sinuosus, A. friedli)* are frequent (Plate 2, Fig. 12). Specimens of Duomostinidae, *Glomospirella* sp., *Gandinella falsofriedli* (Plate 2, Fig. 13), *Endoteba* sp., *Valvulina* sp., *Ophthalmidium* sp. and gymnocodiacean *Asterocalculus heraki* are also present. Some of the bioclasts were subject to blackening (Plate 4, Figs. 4, 5). Lumps and small blackened clasts are also visible. The matrix exhibits a patchy microsparitic alteration. Fenestral pores also occur.

The overlying 110 cm thick bed is dark red and abundant in black pebbles. In the lower part of the bed (Bed 3a) the black clasts are coarser (cm-sized). The typical texture is argillaceous micrite with great amount of unrounded and unsorted lithoclasts, intraclasts. In the studied sample a 10 mm-sized clast of peloidal bioclastic grainstone texture was encountered with gastropods and foraminifera and a number of fenestral pores. Micritization and traces of solution were observed on the margin of this clast (Plate 4, Fig. 7). Blackened *Rivularia*-like calcimicrobe, 1.5 mm in size was also encountered. The other clasts are of probably pedogenic origin; micritic or microsparitic with root casts,

locally. In a 1 mm wide desiccation crack well-preserved thin-shelled ostracods were found in crystal-silt internal sediment (Plate 4, Fig. 6). In the upper part of this bed (Bed 3b) the micritic matrix is rich in 1–2 mm-sized mostly reef-derived bioclasts from Inozoan and Chaetetid sponges, calcimicrobes that are usually bioeroded, micritized and surrounded by a limonitic micrite envelope. Fragments of gastropods, bivalves, crinoids, and aulotortid foraminifera *(Aulotortus friedli, A.* cf. *communis)* also occur. Blackened calcimicrobes were also found. There are a few lithoclasts, abundant in fenestral pores and a number of intraclasts usually with limonitic staining.

The red limestone intercalation is overlain again by light grey limestone beds. The lowermost bed (Bed 4) is made up of peloidal bioclastic grainstone (Plate 4, Fig. 8). It is medium- to coarse-grained calcarenite with fragments of megalodontids and other bivalves, foraminifera (Duostominidae, *Trochammina* spp., *Endoteba* sp.), rivulariaceans and micritized microbial nodules. A few blackened calcimicrobes were also encountered. There are relatively large solution cavities after megalodont shells which are filled by coarse sparry calcite.

The beds of the studied outcrop were deposited in a backreef lagoon where along with the autochthonous carbonate grains, reef-derived, storm-transported bioclasts and lithoclasts were also deposited occasionally. In the foraminifera fauna the *Aulotortus* are predominant; some of them *(Aulotortus communis)* were dweller of the calcarenitic backreef environments whereas others *(A. tenuis, A. friedli)* preferred the protected muddy lagoon. The Duostominids commonly occur in the oncoidal facies (e.g. DULLO, 1980). The features of the red interbed indicate incipient pedogenesis during a subaerial exposure episode. Traces of meteoric diagenesis were encountered in the grey bed below the red one.
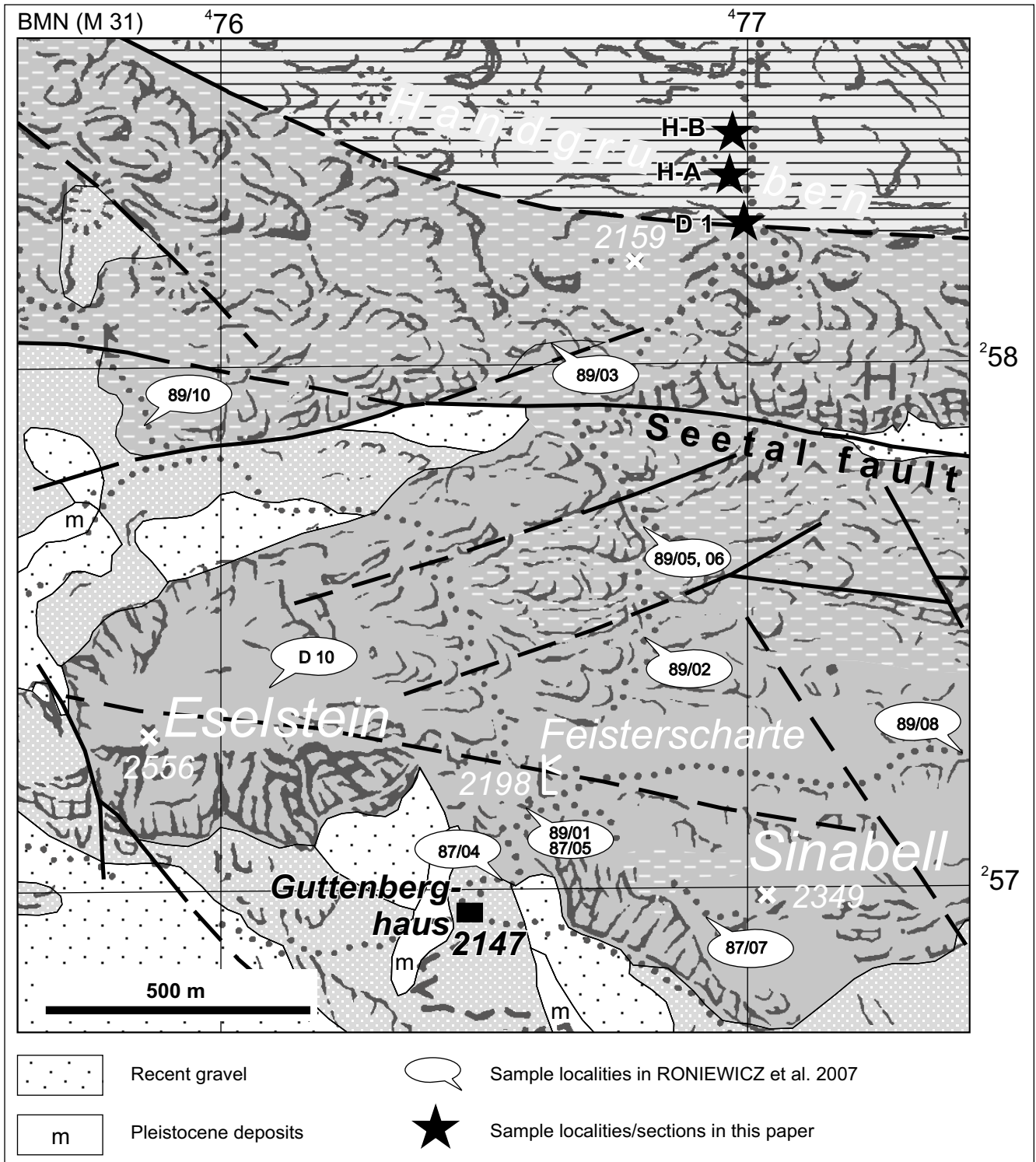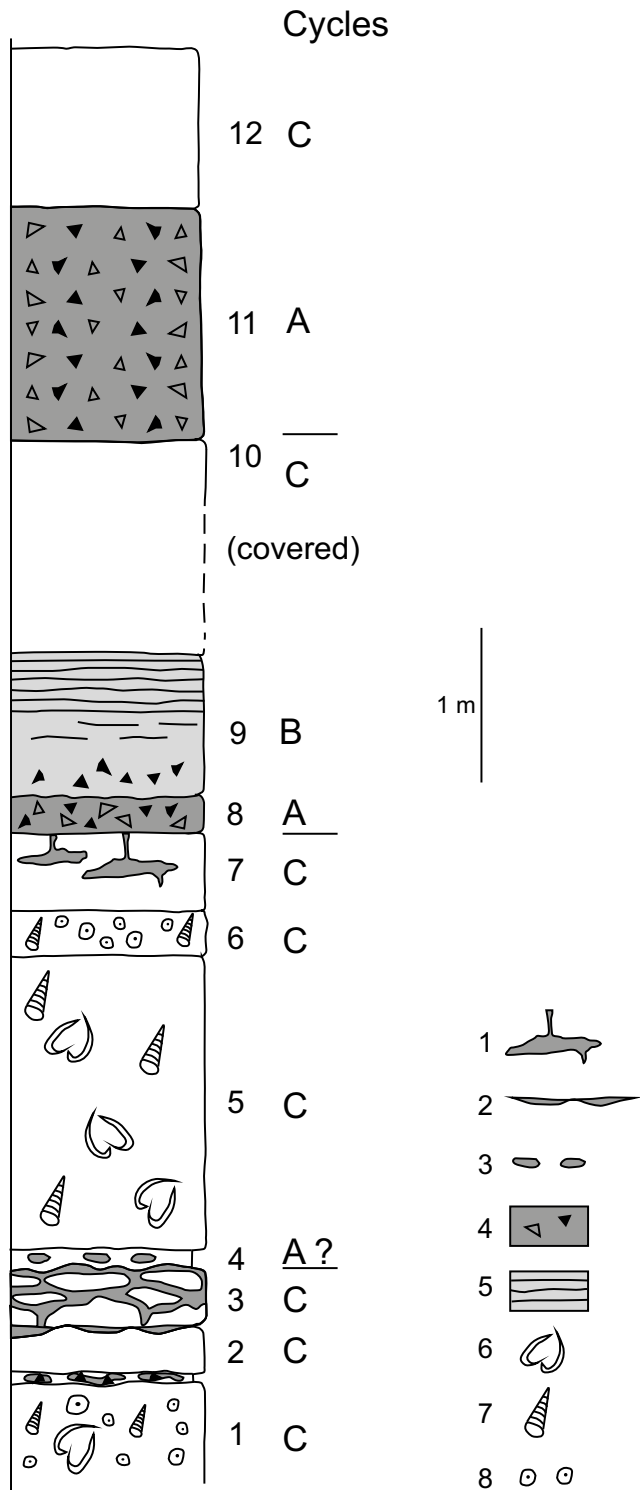
Text-Fig. 3.
Geological map of the Feisterscharte area, showing the studied sections and localities referred to in the text.

Section Handgruben B

Location of the sections studied is shown on Text-Fig. 3 (marked by H–B). On Plate 3, Fig. 2 gently dipping beds of the longer measured section are visible. Text-Fig. 4 displays the lithological column of the section with indication of the facies-types of the beds. The typical microfacies of the beds are presented on Plates 5 and 6.

The lowermost bed of the studied succession is light grey oncoidal limestone with megalodonts and gastro-

pods (Bed 1). It has an oncoidal wackestone texture (Plate 5, Fig. 1). The matrix is peloidal microsparite, locally clotted. The size of oncoids is 1–4 mm. Generally, a lump of clotted microsparite serves as the nucleus of the oncoids (Plate 5, Fig. 2). There are intraclasts (plasticlasts) of peloidal grainstone texture. Centimeter-sized microbial clusters with only a thin microbial crust or without any crust also occur. From among the bioclasts a few, mostly agglutinated foraminifera *(Trochammina* sp., *Valvulina* sp., *Glomospira* sp., *Kaevaria fluegeli* and *Frondicularia wood-*

Cycles

12 C

11 A

10 C

(covered)

9 B

8 A

7 C

6 C

5 C

4 A ?

3 C

2 C

1 C

1 m

1

2

3

4

5

6

7

8

Text-Fig. 4.
Litho- and biofacies characteristics of section Handgruben B.
1 = cavities filled by red limestone;
2 = paleokarst pockets filled by red argillaceous limestone;
3 = reddish patches;
4 = limestone with lithoclasts and black pebbles;
5 = yellowish laminated limestone;
6 = megalodonts;
7 = gastropods;
8 = oncoids.

wardi), microbially encrusted mollusc shell fragments and a cm-sized embryonic ammonite test can be mentioned (Plate 5, Fig. 1). In small cavities formed by burrowing or desiccation micrite fill with thin-shelled ostracods were

encountered. There are solution pores, 0.1–1 mm in size with sparitic lining and crystal silt fill. This bed is capped by a 5 cm thick horizon showing features of paleokarstification. Solution pockets and pipes filled by red argillaceous limestone are visible.

Bed 2 is light grey limestone displaying a vague lamination. The lower part of the studied sample is made up of peloidal micrite-microsparite containing peloidal grainstone plasticlasts. Moulds of thick-shelled bivalves and gastropods, and small sized agglutinated *(Trochammina* sp., Textulariidae sp.) and miliolids *(Agathammina* sp., *Ophthalmidium* sp.) occur. This texture progresses upward into a laminitic one characterised by alternation of micrite and microsparite laminae (Plate 5, Fig. 3). The top of this bed is uneven due to karstic solution; there are pockets with red argillaceous carbonate fill.

Bed 3 consists of light grey limestone that is crosscut by a network of fractures and cavities filled by reddish fill. The texture is peloidal microsparite with small microbial nodules and mm-sized intraclasts. There are some mm-sized oncoids and a few well-preserved agglutinated foraminifera, mainly *Trochammina* spp. Bird's-eye pores are a typical feature of this bed and amalgamation of these pores to a network is also common. Mm- to cm-sized lenticular pores, sheet-cracks formed via desiccation and solution also occur. They often show geopetal fill with crystal silt at the base of the pores, in some cases with ostracods and coarse mosaic sparite above it (Plate 5, Figs. 4, 5).

Bed 4 is light brown limestone with red patches. The sedimentary texture is peloidal wackestone containing tiny peloids and a few foraminifera *(Trochammina* spp.) in a microsparitic matrix (Plate 5, Fig. 6). It is abundant in smaller or larger bird's-eye pores probably of desiccation origin. A 6 mm-sized red pedogenic clast was encountered. There are mm- to cm-sized cavities, usually of irregular rarely tubular shape. Geopetal fill is visible in some of the cavities with peloidal internal sediment (Plate 5, Fig. 7).

Beds 3 and 4 were formed in a shallow subtidal environment that was subsequently affected by desiccation, and karstic solution. Bed 3 was slightly subject to pedogenesis, the tubular cavities are probably root casts.

Bed 5 is of brownish grey colour with megalodonts and gastropods. Tiny black grains were observed in the lower part of the bed. The texture is bioclastic wackestone, abundant in globular biomolds. A few recrystallised involutinids *(Aulotortus tumidus, Aulotortus* sp.) and thin-shelled ostracods could be recognised. There are microbial nodules (Plate 5, Fig. 8) and some intraclasts.

Bed 6 consists of light grey oncoidal limestone with gastropods. Peloidal, bioclastic, oncoidal packstone–grainstone is the typical texture. The oncoids (2–7 mm in size) have no definite nucleus, cemented peloids and bioclasts occur in the inside of the coated grains. Lumps, composite grains are also common. Bioclasts are usually coated by a micrite envelope or microbial crust. Along with foraminifera (Duostominidae spp., *Trochammina* sp.*, Valvulina* sp.*, Glomospira* sp.*, Alpinophragmium perforatum, Aulotortus friedli, Labalina* sp.*, Frondicularia woodwardi, Reophax?* sp.) gastropods (Plate 6, Fig. 2), mollusc and echinodermata fragments and a well preserved dasycladalean alga *Poikiloporella duplicata* were found (Plate 6, Fig. 1). Irregular solution cavities with drusy sparry calcite fill are relatively common.

Bed 7 is of medium grey colour and rich in mm- to cm-sized oncoids (microbially coated microbial nodules) (Plate 6, Fig. 3). It is oncoidal, bioclastic grainstone. The bioclasts are abraded and coated by micrite. Along with calcimicrobes *(Rivularia, Girvanella)*, coral detritus, fragments of thick-shelled bivalves, gastropods, ostracodes a few well-preserved foraminifera *(Triasina hantkeni, Variostoma* sp., Duostominidae, *Valvulina* sp., *Sigmoilina schaeferae, Endoteba* sp.) were encountered (Plate 2, Figs. 15, 17). There are larger pores among the coarse grains, but in some cases the solution enlarged the pores. The pores and solution cavities commonly have geopetal fill. Centimeter-sized karst-related pockets with red carbonate fill also occur.

Bed 8 consists of red argillaceous limestone abundant in mm-sized black and white clasts. The texture displays a patchy pattern with intraclasts and lithoclasts (Plate 6, Fig. 4). In the micritic matrix there are fragments of molluscs, corals, thin-shelled ostracods and foraminifera *(Aulotortus impressus, Valvulina* sp., *Nodosaria* sp.). Mudstone lithoclasts and a larger wackestone clast with bird's-eye pores occur as well. There are a number of microsparitic clasts and globular grains with limonitic coating.

The lower part of Bed 9 is light grey limestone with scattered tiny black clast. The upper part of the bed is yellowish and laminated. The sample taken from the upper part clearly shows that the laminae are made up of fine calcarenite grainstone. Some of the laminae are graded suggesting storm-related tidal flat deposition. Peloids and biomolds are abundant; fragments of bivalves, foraminifera and *Rivularia*-type calcimicrobes are the recognisable bioclasts. Among the foraminifera specimens of *Aulotortus friedli* are relatively frequent, besides them other Aulotortidae *(A. impressus, A. tumidus, A. tenuis)* (Plate 2, Figs. 18, 19), *Sigmoilina schaeferae, Agathammina austroalpina* and *Trochammina* sp. also occur. There are tiny spar-filled pores of irregular shape (Plate 6, Fig. 5). Sheet cracks parallel to the lamination are common. They have usually an uneven roof and complex geopetal filling with micrite, microsparite in the basal part and isopach sparite cement above it (Plate 6, Fig. 6).

Bed 10 is light grey limestone with small bioclasts. It is characterised by peloidal microsparite texture with bioclasts usually in micrite envelope. Foraminifera are common; taxa in order of frequency are *Trochammina* sp., *Aulotortus friedli, Endoteba* spp., *Diplotremina* sp., *Tetrataxis inflata* (Plate 2, Fig. 14), *Frondicularia woodwardi* and *Galeanella panticae* (Plate 2, Fig. 16). Fragments of echinoderms, *Tubiphytes, Rivularia*-type calcimicrobes (Plate 6, Fig. 7), *Thaumatoporella* also occur sporadically. There are a number of tiny solution vugs with sparitic fill and larger bird's-eye pores. Circumgranular cement was observed around larger peloids.

Bed 11 is dark red aphaneritic limestone with a number of small blackened and non-blackened clasts. The original depositional texture of the rock cannot be recognised due to the pedogenic alteration. In the peloidal micritic matrix there are a few mollusc shell fragments and foraminifera *(Aulotortus friedli,* Aulotortidae indet., *Endoteba* sp., *Nodosaria* sp.). Several intraclasts were found which are made up of micrite containing thin-shelled ostracods and small pores with microsparitic fill. Fenestral pores of various sizes typify the entire sample (Plate 6, Fig. 8). The pores usually have geopetal fill with crystal silt internal sediment. Fractures with similar fill were also observed. There are alveolar structures and root cast shaped larger pores.

The topmost bed of the measured section (Bed 12) is light grey fine crystalline limestone.

Based on field observations and microfacies studies, it is plausible that the succession is cyclic. It shows the basic characteristics of the Lofer cycles since the succession is made up of alternation of subtidal and peritidal beds. The subtidal beds are usually oncoidal and contain megalodonts, gastropods and foraminifera. Among the foraminifera the *Aulotortus communis, Tetrataxis* and Duostominidae preferred the calcarenitic substrate whereas *Aulotortus tenuis, A. friedli, Trochammina, Agathammina* were inhabitants of the muddy lagoonal environments (e.g. SCHÄFER & SENOWBARI-DARYAN, 1978; DULLO, 1980). Appearance of *Sigmolinia schaeferae* in Bed 9 suggests redeposition of some skeletal material from the reef zone (BERNECKER, 1996).

Some of the subtidal beds were affected by pedogenic alteration, karstification and meteoric early diagenesis. There are beds, which probably deposited on the tidal flat. The shallow subtidal carbonate factory may have been the source of the carbonate mud also in these cases but these beds having usually reddish colour also contain reworked soil derived material and were also affected by incipient pedogenesis. Laminated structure of Bed 9 reflects storm deposition in the supratidal zone. Based on these features the beds of the studied succession correspond with FISCHER'S (1964) facies units (A, B and C facies) and the Lofer cycles are recognisable (Text-Fig. 4).

The foraminifera fauna may provide tools for the chronostratigraphic evaluation of the Handgruben sections. Some of the determined species have a long stratigraphic range (Upper Triassic or even Middle to Upper Triassic). There are some species probably of Norian to Rhaetian range, although their assignment is commonly debated. Examples are listed below. *Alpinophragmium perforatum*: Norian–Rhaetian (FLÜGEL, 1967), Norian (WURM, 1982); *Aulotortus communis*: Norian–Rhaetian (KOEHN-ZANINETTI, 1969); *Aulotortus impressus*: Rhaetian (KRISTAN-TOLLMANN, 1964), Lower Rhaetian (SALAJ & STRANIK, 1970), Rhaetian (PANTIČ-PRODANOVIĆ & RADOŠEVIĆ, 1981), Norian–Rhaetian (KOEHN-ZANINETTI, 1969), Carnian–Rhaetian (SALAJ et al., 1983); *Aulotortus sinuosus*: Norian (WURM, 1982), Rhaetian (KRISTAN-TOLLMANN, 1964), Norian–Rhaetian (KOEHN-ZANINETTI, 1969; PANTIČ-PRODANOVIĆ & RADOŠEVIĆ, 1981; DE CASTRO, 1990); *Aulotortus tenuis*: Rhaetian (KRISTAN-TOLLMANN, 1964), Norian–Rhaetian (KOEHN-ZANINETTI, 1969; PANTIČ-PRODANOVIĆ & RADOŠEVIĆ, 1981), Ladinian? Norian–Rhaetian (SENOWBARI-DARYAN et al., 2010); *Aulotortus tumidus* (KRISTAN-TOLLMANN, l964): Rhaetian (KRISTAN-TOLLMANN, 1964), Lower Rhaetian (SALAJ & STRANIK, 1970), Norian–Rhaetian (KOEHN-ZANINETTI, 1969; PANTIČ-PRODANOVIĆ & RADOŠEVIĆ, 1981), Norian (WURM, 1982), Upper Triassic–Liassic? (SENOWBARI-DARYAN et al., 2010); *Gandinella falsofriedli*: Upper Norian – Lower Rhaetian (POISSON et al., 1985), Upper Alaunian – Sevatian (SALAJ et al., 1988), Upper Norian – Rhaetian (ZAMPARELLI et al., 1995); *Sigmoilina schaeferae*: Norian–Rhaetian (SCHÄFER & SENOWBARI-DARYAN, 1978); *Triasina hantkeni*: Norian–Rhaetian (BERNECKER, 2005), Upper Norian – Lower Rhaetian *(Rhabdoceras suessi* zone – *Choristoceras marshi* zone – DE CASTRO, 1990); *Turrispirillina minima*: Norian–Rhaetian (SALAJ et al., 1983), Norian (ORAVECZ-SCHEFFER, 1987).

To summarize, on the basis of the foraminifera fauna the layers exposed in the Handgruben sections are probably

41

of Late Norian to early Rhaetian age. Since there is no in-dex foraminifera taxon for distinguishing the Upper Norian from Lower Rhaetian we cannot make more detailed bios-tratigraphically constrained assignment. On the basis of the geological setting of the section, and taking into ac-count the general dip of the strata, the Upper Norian as-signment seems to be more realistic (Text-Fig. 2).

Comparison with Sections Representing the Platform Interior

In the last years several Lofer cyclic Dachstein Lime-stone sections were studied on the northern part of the Dachstein plateau (Krippenstein-Schutzhaus and Gretl-Rast sections) 5–6 km northward to the presently stud-ied outcrops (Haas et al., 2007, 2009). Based on the foraminifera fauna both sections are Norian, probably Up-per Norian (Haas et al., 2009). Paleogeographically those sections represent the internal part of the Dachstein plat-form, far from the marginal reef tract (Mandl, 2000). So it is not amazing that there are significant differences in the basic characteristics of the cyclic successions near and far from the platform margin. In the section Handgruben B, the oncoidal facies is typical in the subtidal C facies. The A facies is relatively thick, and typified by the presence of reworked soil-derived clasts. The B facies is poorly deve-loped, and no stromatolites were found.

In the sections studied near Mt. Krippenstein, in the north-ern part of the Dachstein plateau (Haas et al., 2007) the main characteristics of the Lofer cycles can be summa-rized as follows. The boundaries of the cycles are usually erosional disconformities showing features of karstifica-tion. Member A that is typically reddish or greenish argil-laceous limestone is a few mm to 10 cm thick. It can be interpreted as tidal flat deposit consisting predominantly of subtidal carbonate mud redeposited by storms. It was mixed with reworked air borne fine carbonate particles and argillite that were accumulated and subjected to weath-ering on the subaerially exposed platform. Rip-ups from consolidated sediment, blackened intraclasts and skele-tons of tidal flat biota may have also contributed to the material of facies A. The karstic solution pockets and cavi-ties are commonly filled by the A facies. In micritic cavity-fills low-salinity to freshwater ostracods were encountered (Haas et al., 2007).

The basal disconformity or the A facies is usually followed by white to light yellow or darker grey stromatolites or mudstones with fenestral pores, sheet cracks and shrink-age cracks, showing features of member B. The thickness of member B is usually 10–50 cm but may exceed 1 m, rarely. The B facies can be interpreted as intertidal to lower supratidal tidal flat deposit. The B or rarely the A facies is overlain by light brown or greyish brown, light grey lime-stone commonly with megalodonts, i.e. member C. The typical microfacies is peloidal, bioclastic wackestone, packstone or grainstone with foraminifera (involutinids, nodosariids), fragments of dasycladalean algae, molluscs, echinoderms (Haas et al., 2007, 2009). The thickness of member C is 1–3 m.

In the studied sections the ABC facies succession was found at the base of many cycles suggesting a transgres-sive trend. In contrast, the regressive part of the cycles is frequently missing due to the post-depositional truncation.

The facies differences between the marginal and the inter-nal cyclic successions can be summarized as follows.

1. Above the erosional, karstic disconformity surface the A facies appear to be thicker in the marginal zone (Hand-gruben section) where traces of the in situ pedogenesis could also be observed.

2. The B facies (stromatolites, loferites) are usually present at the basal part of the cycles in the platform interior succession (Krippenstein), whereas similar facies (lami-nated mudstone but not stromatolite) was found only in a single cycle in the studied marginal succession.

3. The C facies is typically oncoidal packstone, grainsto-ne in the marginal zone and peloidal bioclastic wacke-stone, packstone and grainstone in the platform interior area; megalodonts are common in both.

These differences probably reflect the differences in the paleogeographic setting. In the marginal zone, near the offshore edge of the platform oncoid shoals developed un-der relatively high-energy conditions above the fair-weath-er wave base. The marginal patch-reefs (knoll-reefs) may have been situated somewhat deeper. The wide platform interior area was located behind the marginal shoals and during the high sea level periods it was slightly deeper than the oncoid mounds. The sea-level drops led to sub-aerial exposure and related karstification both of the shoal belt and the interior lagoon. Rising sea level led to the es-tablishment of tidal flat conditions on the platform interior whereas the subaerial conditions were prolonged on the slightly elevated previous shoals which resulted also in in-cipient pedogenesis.

Comparison with the Oncoidal Dachstein Limestone in the Transdanubian Range

In the Transdanubian Range (TR), Hungary, the Dach-stein-type platform carbonates developed in a remarkable areal extension and great thickness. Paleogeographically this area was a segment of the Neotethys shelf which was located between the South Alpine and the Upper Aust-roalpine domain. Upfilling of the intraplatform basins by the latest Carnian made possible the establishment of the large platform. The facies polarity is straightforward; the NE part of the TR represents the offshore platform margin whereas its SW part was closer to the firm land (Haas & Budai, 1995). Over the predominant part of TR the plat-form carbonates are definitely cyclic showing characte-ristics of the Lofer cyclicity (Haas, 2004). The lower part (Upper Tuvalian to Middle Norian) of the cyclic succession is pervasively dolomitized, the upper part (Upper Norian to Rhaetian) is non-dolomitized, and there is a transition-al interval between them. However, in the NE part of TR (Buda Hills, blocks in the eastern side of the Danube) the intraplatform basins developed in the Carnian preserved during the Late Triassic and on the smaller isolated plat-forms thick-bedded oncoidal limestones (the oncoidal facies of the Dachstein Limestone) and locally patch reefs were formed.

In the central part of the Buda Hills the Late Carnian to Early Norian cyclic dolomites (corresponding to the Dach-stein Dolomite) is overlain by the oncoidal development of the Dachstein Limestone. It is typified by predominance

of the oncoidal-oolitic grainstone subtidal facies (C facies) with megalodonts and gastropods. It is punctuated by disconformity surfaces, but the peritidal facies (member A and B) are scarce and thin. It means that the Lofer cyclicity is only rudimentary, amalgamation of the elementary cycles is common (Haas, Ed., 2004).

In the blocks on the east side of the Danube (Nézsa–Csővár block), Late Carnian patch-reefs are known that are made up of calcareous sponges, various encrusting organisms, calcimicrobes and a few corals (Kovács, 2004). In some places it is well visible that the reef patches are surrounded by oncoidal limestone. The higher, Norian part of the thick-bedded limestone is made up predominantly of oncoidal-oolitic grainstone akin to that in the Buda Hills. The lower part of the several hundred meters thick succession consists mostly of subtidal facies, the A facies is missing; the B facies is thin and typified either by fenestral laminated sheet-crack or stromatolite rip-up facies (Balog & Haas, 1990).

Comparing the oncoidal facies of the Dachstein Limestone in the southern part of the Dachstein plateau and the NE part of the TR it is plausible that both occur near the platform margin. In the case of the Dachstein plateau it is a relatively narrow belt, whereas in the TR it seems to be much wider. However, according to the relevant paleogeographic models (Mandl, 2000) the platform of the Dachstein plateau was in direct connection with the deep shelf basin of the Neotethys Ocean, whereas the platform margin was more articulated in the segment of the TR, where intraplatform basins existed among smaller platforms (Haas, 2002). In the area of the Dachstein plateau the oncoidal zone may have been relatively elevated and that may be the cause of the striking paleokarst features and well-developed supratidal A facies which developed during the low sea-levels. In contrast, in the area of the NE part of the TR, the subaerial exposure surfaces and the peritidal facies are frequently missing, there are amalgamated cycles, that means that the area remained inundated even during the sea-level lowstands.

Acknowledgements

Plate 1

Microfacies characteristics of massive limestones of reef and near-reef facies

Fig. 1: Reef derived breccias with sparitic cement. A coral fragment with microbial crust is visible in the left side.

Fig. 2: Fragments of microbial crusts and lithoclasts, surrounded by sparry calcite cement.

Fig. 3: Calcareous sponge fragment.

Fig. 4: Rivulariacean fragment.

Fig. 5: Encrusting foraminifera *Tolypammina gregaria*.

Fig. 6: Bioclasts and lithoclasts bounded by encrusting foraminifera *Alpinophragmium perforatum*.

Fig. 7: Domal microbial crust.

Fig. 8: Microproblematicum *Baccanella floriformis*.
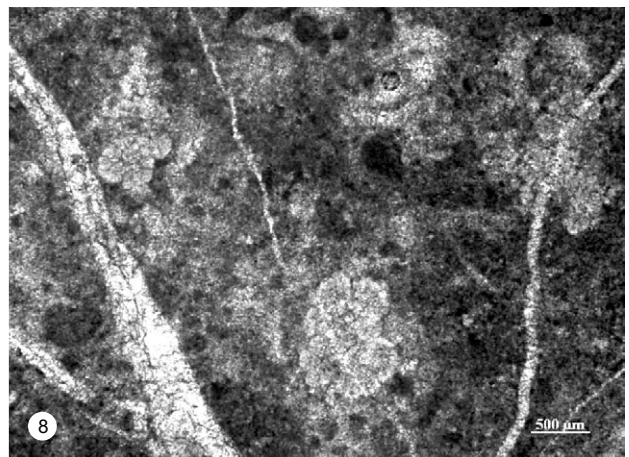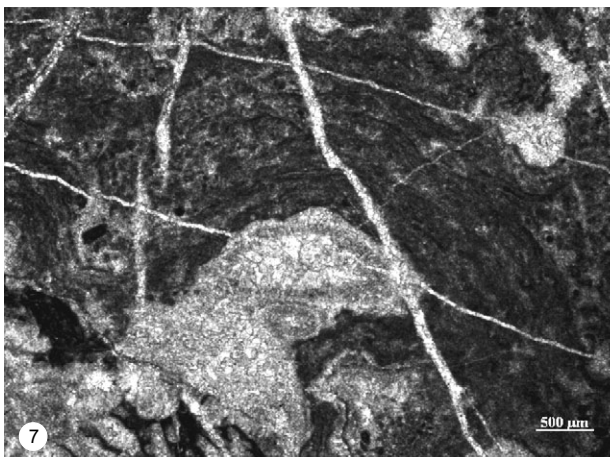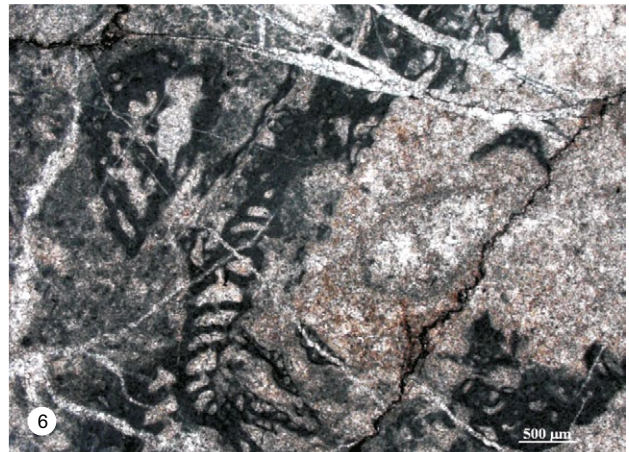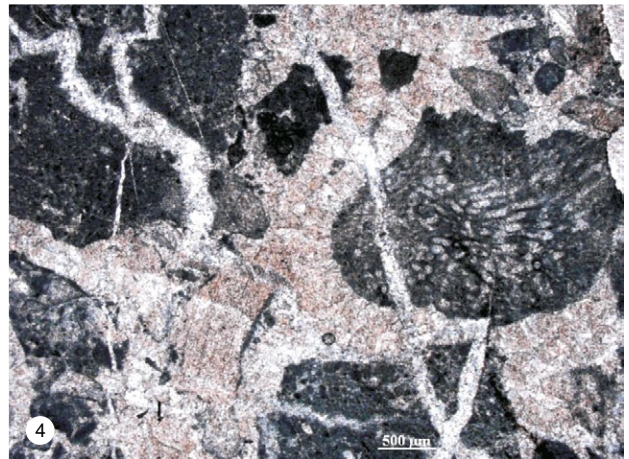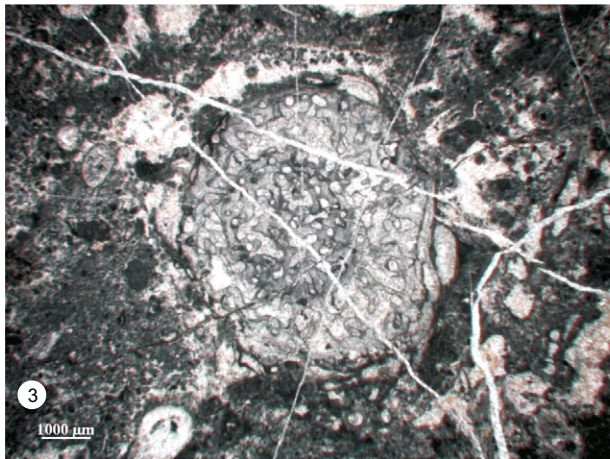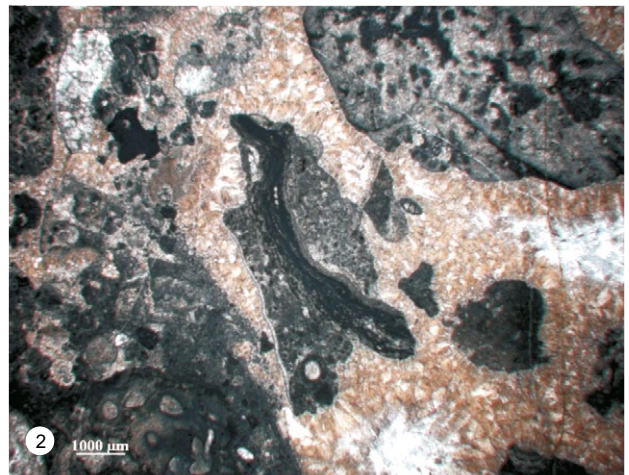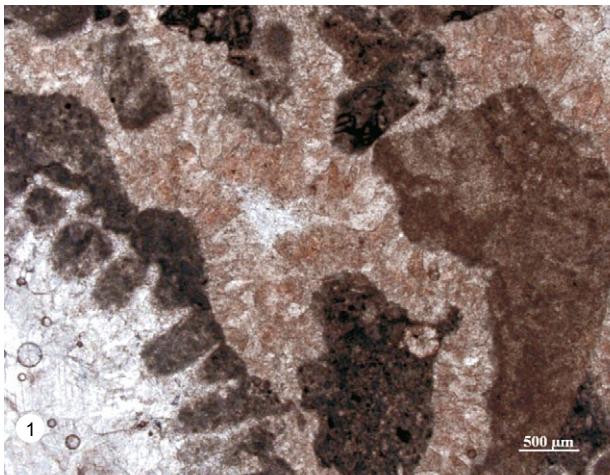
Plate 2

Foraminifera and microproblematica in the studied exposures

Figs.   1–5: Samples taken south to the Seetal Fault.

Fig.   1: *Miliolipora cuvillieri*.

Fig.   2: *Miliolipora cuvillieri*.

Fig.   3: *Ophthalmidium triadicum.*

Fig.   4: *Kaevaria fluegeli.*

Fig.   5: *Agathammina austroalpina.*

Figs.   6–7: Sample D1.

Fig.   6: Duostominidae.

Fig.   7: *Messopotamella angulata.*

Figs. 8–11: Section Handgruben A Bed 1.

Fig.   8: *Aulotortus sinuosus*.

Fig.   9: *Aulotortus impressus.*

Fig.   10: *Aulotortus communis.*

Fig.   11: *Aulotortus friedli.*

Figs. 12–13: Section Handgruben A, Bed 2.

Fig.   12: *Aulotortus friedli.*

Fig.   13: *Gandinella falsofriedli.*

Figs. 14–19: Section Handgruben B.

Fig.   14: *Tetrataxis inflata,* Bed 10*.*

Fig.   15: *Sigmoilina schaeferae,* Bed 7*.*

Fig.   16: *Galeanella panticae* and *Trochammina* sp., Bed 10.

Fig.   17: *Triasina hantkeni,* Bed 7*.*

Fig.   18: *Aulotortus tumidus* Bed 9.

Fig.   19: *Aulotortus tenuis* Bed 9.

200µ
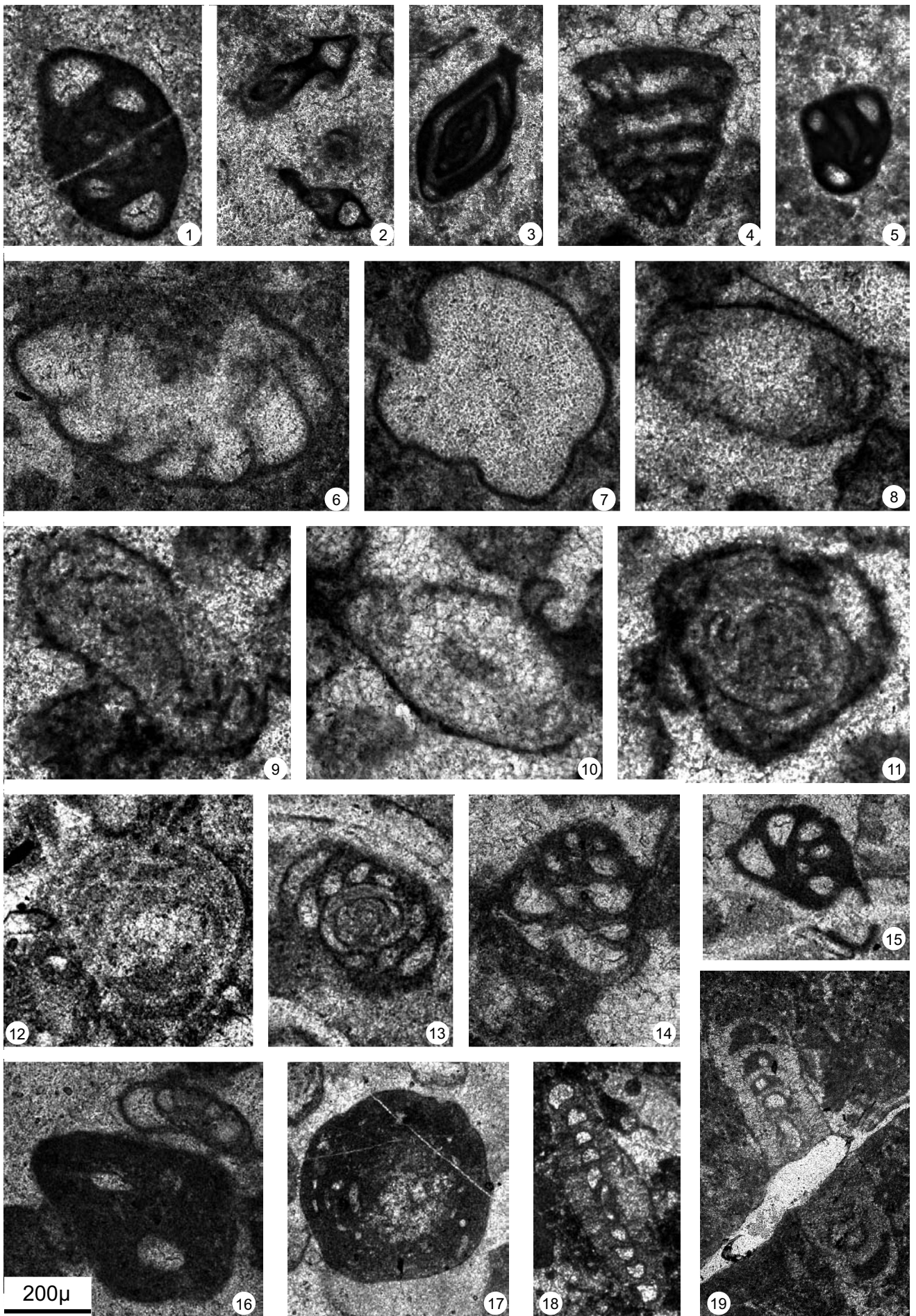
Plate 3

Measured and studied sections with numbers of the measured and sampled beds

Fig. 1: Section Handgruben A.

Fig. 2: Section Handgruben B.

Plate 4

Microfacies characteristics of section Handgruben A

Fig. 1: Peloidal, bioclastic (dasycladalean) grainstone; the intra- and intergranular pores and solution vugs are filled by bladed and drusy calcite cement (Bed 1).

Fig. 2: Peloidal, bioclastic grainstone with fragments of dasycladalean algae, bivalves and an embryonic ammonite (Bed 1).

Fig. 3: Fragments of bivalves, gastropods, and calcareous algae. The shelter pores are filled by isopach sparite cement (Bed 1).

Fig. 4: Peloidal microsparite with fragments of blackened (brown in thin section) Rivulariaceans. The small solution pores are filled by fine mosaic cement (Bed 2).

Fig. 5: Peloidal, bioclastic microsparite with blackened Foraminifera *(Aulotortus communis)* and other bioclasts (Bed 2).

Fig. 6: Pedogenic calcrete; red argillaceous micrite with lithoclasts. A shrinkage crack filled by ostracod-bearing microsparite is visible in the middle of the picture (Bed 3a).

Fig. 7: Peloidal bioclastic grainstone lithoclast in red argillaceous micrite matrix (Bed 3a).

Fig. 8: Peloidal bioclastic grainstone with fragments of Rivulariaceans and bivalves (Bed 4).
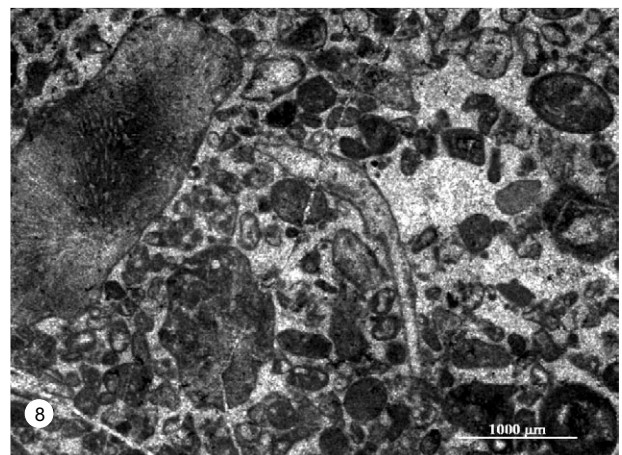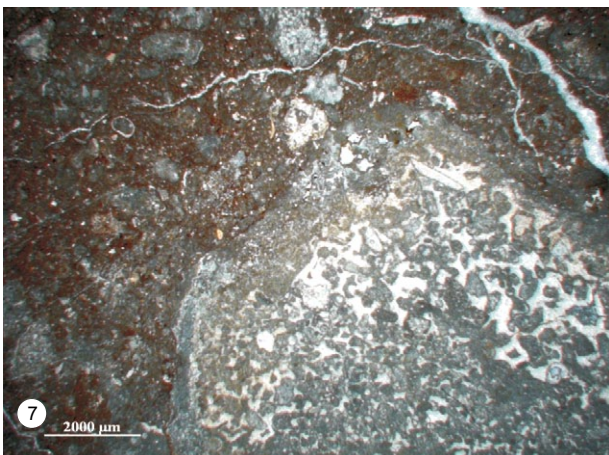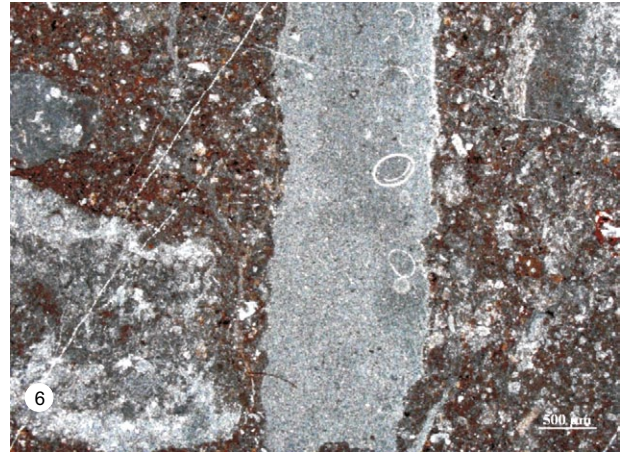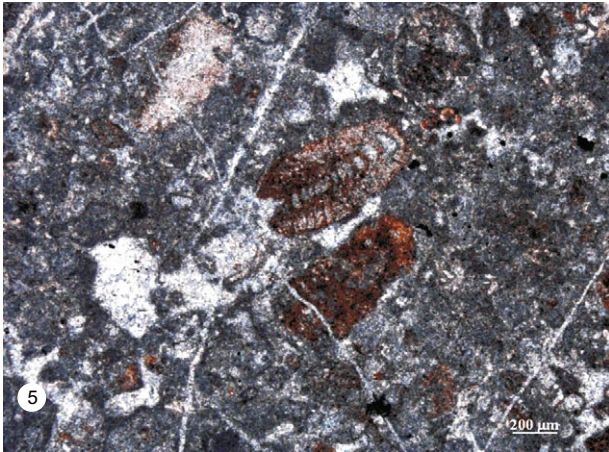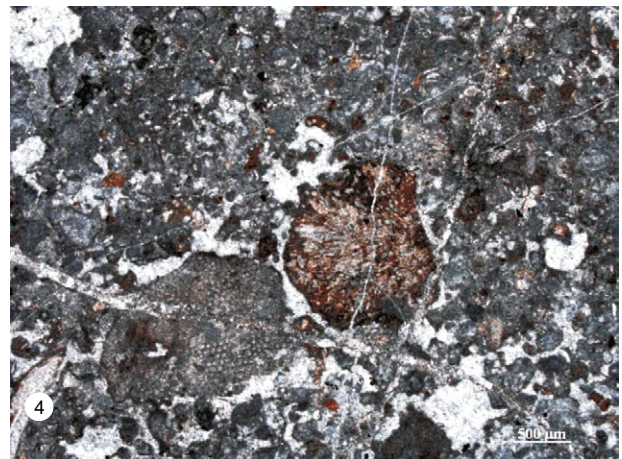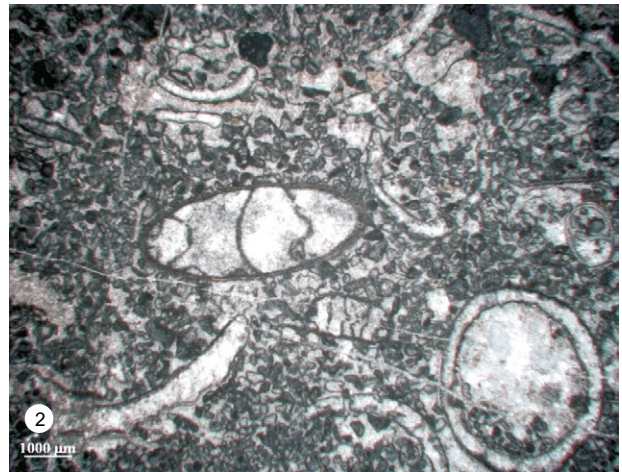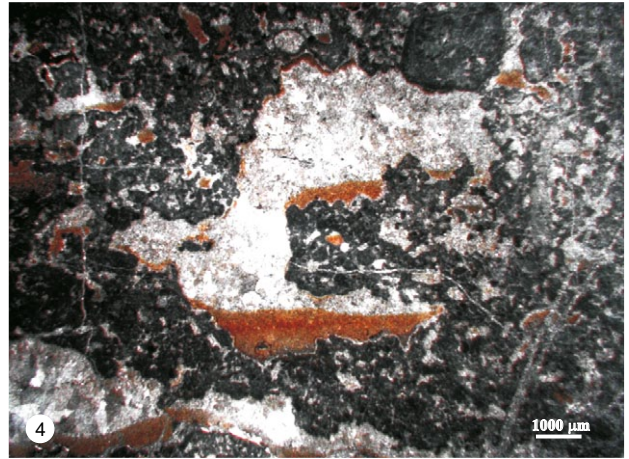
Plate 5

Microfacies characteristics of section Handgruben B

Fig. 1: Oncoidal wackestone with an embryonic ammonite test (Bed 1).

Fig. 2: A lump of clotted peloidal microsparite serves as the nucleus of an oncoid (Bed 1).

Fig. 3: Peloidal micrite progresses upward to laminitic texture (Bed 2).

Fig. 4: Bird's-eye pore with geopetal fill; amalgamation of the pores is well visible (Bed 3).

Fig. 5: A network of the bird's-eye pores; some of them are partially filled by red crystal silt (Bed 3).

Fig. 6: Peloidal wackestone with bird's-eye pores (Bed 4).

Fig. 7: Solution cavity with geopetal fill; peloidal internal sediment occurs at the base of the cavity (Bed 4).

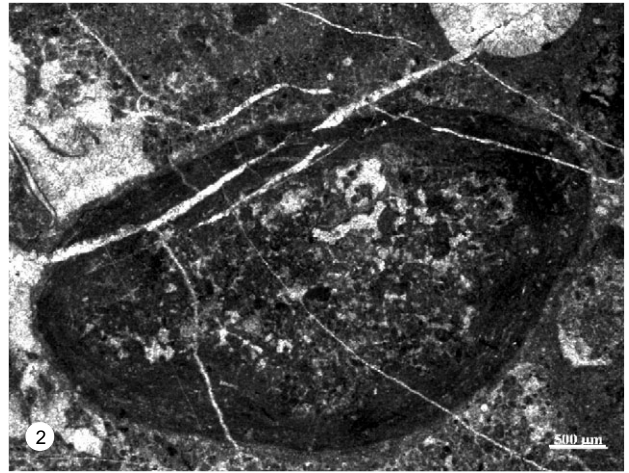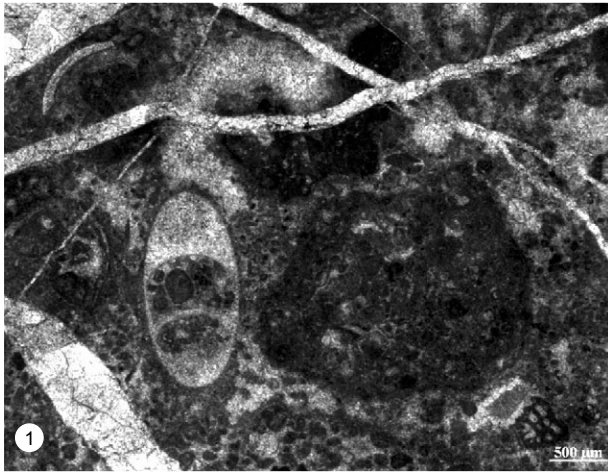Fig. 8: Fragment of calcimicrobial remains in peloidal wackestone (Bed 5).
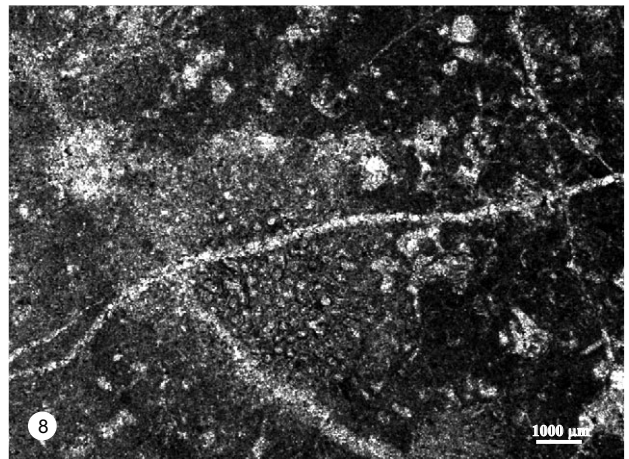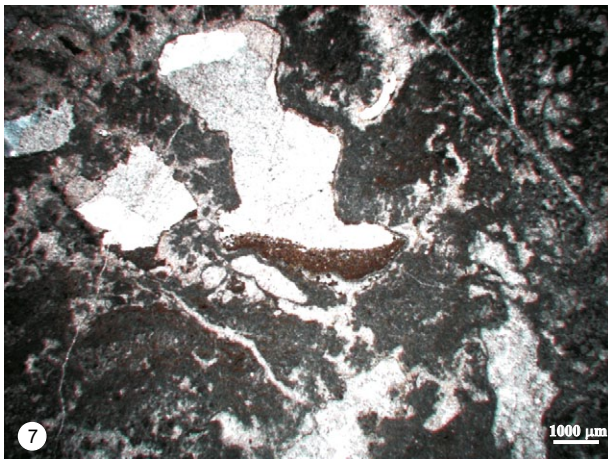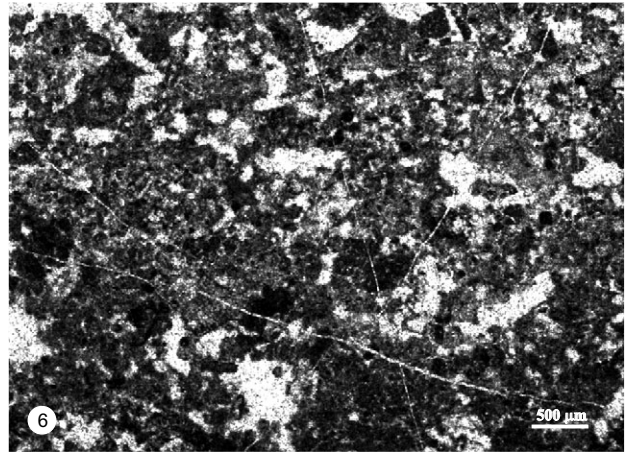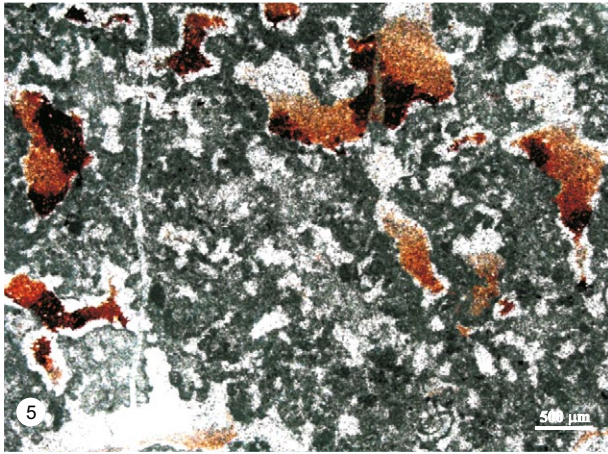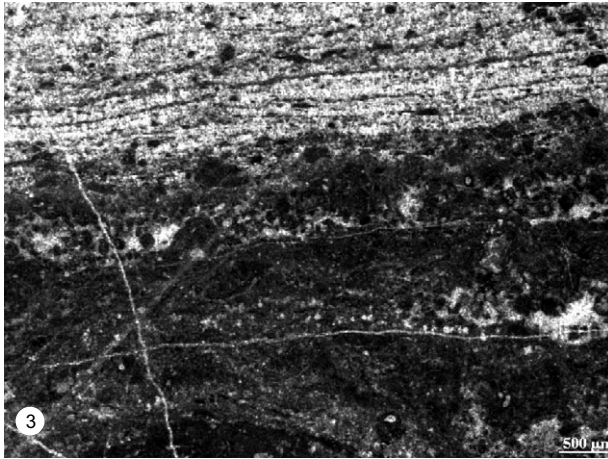
Plate 6

Microfacies characteristics of section Handgruben B

Fig. 1: Fragment of dasycladalean algae *(Poikiloporella duplicata)* in peloidal, bioclastic, oncoidal packstone (Bed 6).

Fig. 2: Microbially encrusted gastropod (Bed 6).

Fig. 3: Microbially coated microbial nodule (Bed 7).
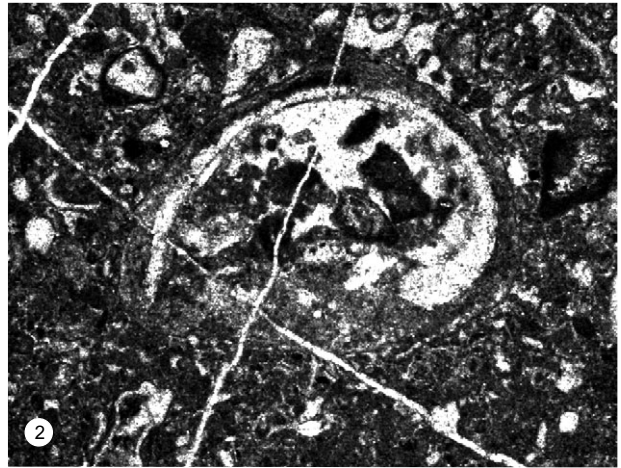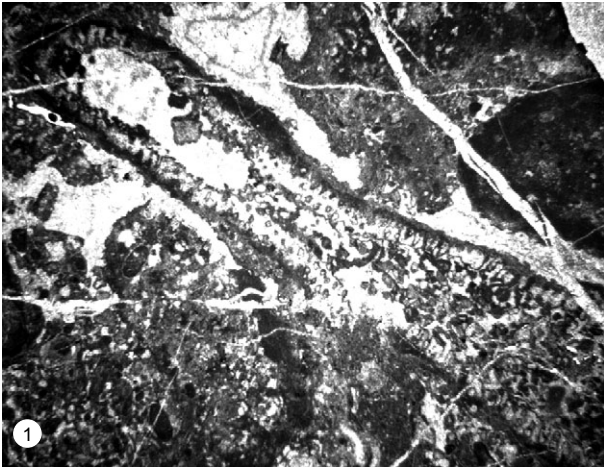
Fig. 4: Small intraclasts and lithoclasts in microsparitic matrix (Bed 8).

Fig. 5: Network of solution vugs with geopetal fill in some of the pores (Bed 9).

Fig. 6: Lenticular solution pore with geopetal fill (Bed 9).

Fig. 7: Peloidal microsparite with a *Rivularia*-type calcimicrobe fragment (Bed 10).

Fig. 8: Peloidal, bioclastic texture, rich in irregular fenestral pores (Bed 11).
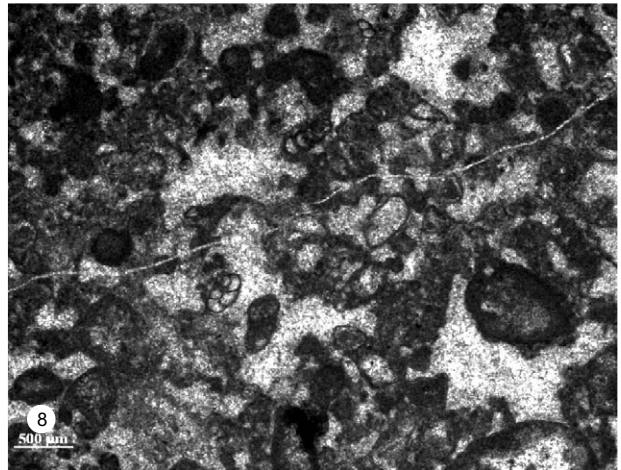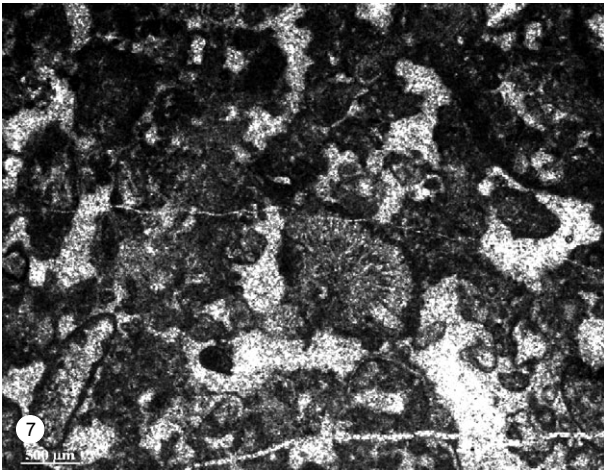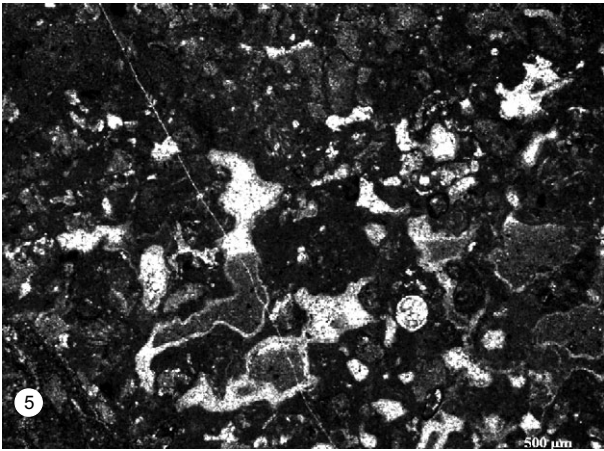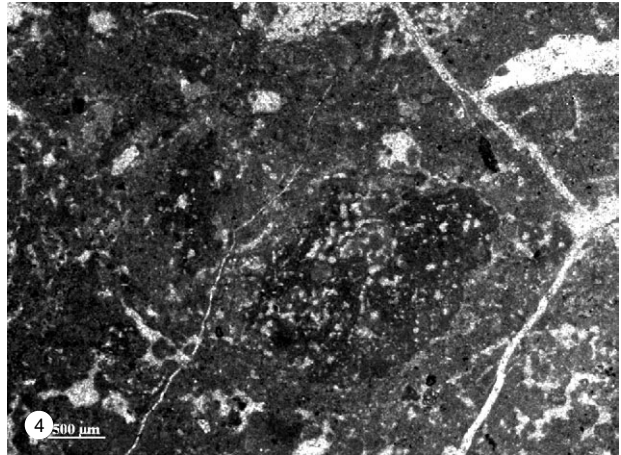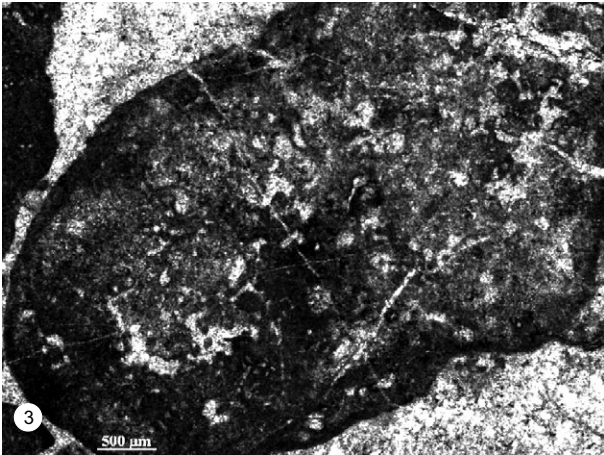
References

BALOG, A. & HAAS, J. (1990): Sedimentological features and diagenesis of the Dachstein Limestone of the Nagyszál Mt. at Vác. – Földtani Közlöny, **120**, 11–18, Budapest.

BERNECKER, M. (1996): Upper Triassic Reefs of the Oman Mountains: Data from the South Tethyan Margin. – Facies, **34**, 41–76, Erlangen.

BERNECKER, M. (2005): Late Triassic reefs from the Northwest and South Tethys. – Facies, **51**, 442–453, Berlin – Heidelberg.

DE CASTRO, P. (1990): Studies on the Triassic carbonates of the Salerno province (Southern Italy): the Croci d'Acerno sequence. – Bolletino della Societa Paleontologica Italiana, **109**, 181–217, Modena.

DULLO, W.-C. (1980): Paläontologie, Fazies und Geochemie der Dachstein-Kalke (Ober-Trias) im südwestlichen Gesäuse, Steiermark, Österreich. – Facies, **2**, 55–122, Erlangen.

FISCHER, A.G. (1964): The Lofer cyclothems of the Alpine Triassic. – Kansas Geol. Surv. Bull., **169**, 107–149, Lawrence.

FLÜGEL, E. (1967): Eine neue Foraminifere aus den Riffkalken der nordalpinen Ober-Trias: *Alpinophragmium perforatum* n. g., n. sp. – Senckenbergiana Lethaea, **48**, 381–480, Frankfurt.

GAŹDZICKI, A. (1983): Foraminifers and Biostratigraphy of Upper Triassic and Lower Jurassic of the Slovakian and Polish Carpathians. – Palaeontologia Polonica, **44**, 109–169, Warszawa.

HAAS, J. & BUDAI, T. (1995): Upper Permian – Triassic facies zones in the Transdanubian Range. – Rivista Italiana Paleontologia e Stratigraphia, **101**/3, 249–266, Milano.

HAAS, J. (2002): Origin and evolution of Late Triassic backplatform and intraplatform basins in the Transdanubian Range, Hungary. – Geologica Carpathica, **53**/3, 159–178, Bratislava.

HAAS, J. (2004): Characteristics of peritidal facies and evidences for subaerial exposures in Dachstein-type cyclic platform carbonates in the Transdanubian Range, Hungary. – Facies, **50**, 263–286, Berlin – Heidelberg.

HAAS, J. (Ed.) (2004): Triász – Magyarország geológiája (Triassic – Geology of Hungary). – 384 p., Budapest.

HAAS, J., LOBITZER, H. & MONOSTORI, M. (2007): Characteristics of the Lofer cyclicity in the type locality of the Dachstein Limestone (Dachstein Plateau, Austria). – Facies, **53**, 113–126, **Berlin – Heidelberg**.

HAAS, J., PIROS, O., GÖRÖG, Á. & LOBITZER, H. (2009): Paleokarst phenomena and peritidal beds in the cyclic Dachstein limestone on the Dachstein Plateau (Northern Calcareous Alps, Upper Austria). – Jb. Geol. B.-A., **149**, 7–21, Wien.

HOHENEGGER, J. & LOBITZER, H. (1971): Die Foraminiferen-Verteilung in einem obertriadischen Karbonatplattform-Becken-Komplex der östlichen Nördlichen Kalkalpen. – Verh. Geol. B.-A., **1971**/3, 458–485, Wien.

HOHENEGGER, J. & PILLER, W. (1975): Ökologie und systematische Stellung der Foraminiferen im gebankten Dachsteinkalk (Obertrias) des nördlichen Toten Gebirges (Oberösterreich). – Palaeogeography, Palaeoclimatology, Palaeoecology, **18**, 241–276, Amsterdam.

KOEHN-ZANINETTI, L. (1969): Les Foraminifères du Trias de la région de l'Almtal (Haute-Autriche). – Jb. Geol. B.-A., Sonderband **14**, 155p., Wien.

KOVÁCS, B. (2004): Paleontological and carbonate sedimentological study of the Upper Triassic formations in the environs of Nézsa. – Diploma work. Eötvös Loránd University (manuscript, in Hungarian).

KRISTAN-TOLLMANN, E. (1964): Beiträge zu Mikrofaunen das Rhät. II. Zwei charakterische Foraminiferengemeinschaften aus Rhätkalken. – Mitt. Ges. Geol. Bergbaustud. Österr., **14**, 135–147, Wien.

KRYSTYN, L., MANDL, G.W. & SCHAUER, M. (2009): Growth and termination of the Upper Triassic platform margin of the Dachstein area (Northern Calcareous Alps, Austria). – Austrian Journal of Earth Sciences, **102**, 22–33, Vienna.

LEIN, R. (1987): Bericht 1986 über geologische Aufnahmen in den Kalkalpen auf Blatt 127 Schladming. – Jb. Geol. B-A., **130**/3, 319–321, Wien.

MANDL, G.W. & MATURA, A. (1995): Geologische Karte der Republik Österreich, 1:50.000, Blatt 127 Schladming. – Wien.

MANDL, G.W. (2000): The Alpine sector of the Tethyan shelf – Examples of Triassic to Jurassic sedimentation and deformation from the Northern Calceareous Alps. – Mitt. Österr. Geol. Ges., **92** (1999), 61–78, Wien.

MANDL, G.W. (2001): Geologie der Dachsteinregion. – In: SCHEIDLEDER, A., BOROVICZENY, F., GRAF, W., HOFMANN, Th, MANDL, G.W., SCHUBERT, G., STICHLER, W., TRIMBORN, P. & KRALIK, M.: Pilotprojekt „Karstwasser Dachstein". Band 2: Karsthydrologie und Kontaminationsrisiko von Quellen – Archiv f. Lagerst.forsch. Geol. B.-A., **21**, 13–37, 2 Beil. (geol. Kt., Profilschnitte), Wien.

ORAVECZ-SCHEFFER, A. (1987): Triassic foraminifers of the Transdanubian Central Range. – Geol. Hung. Ser. Pal., **50**, 331p., Budapest.

PANTIČ-PRODANOVIĆ, S. & RADOŠEVIĆ, B. (1981): Some characteristics of Triassic sediments in the area of Muretenica (Zlatibor Mt. Yugoslavia). – Bulletin du Muséum d'Histoire Naturelle, Série A, **36**, 71–101, Paris.

POISSON, A., CIARAPICA, G., CIRILLI, S. & ZANINETTI, L. (1985): *Gandinella falsofriedli* (SALAJ, BORZA ET SAMUEL, 1983) (Foraminifere, Trias supérieur), étude de l'espèce sur la base du materiel-type de Domuz Dag (Taurus Lycien, Turquie). – Revue de Paléobiologie, **4**, 133–136, Genève.

RONIEWICZ, E., MANDL, G.W., EBLI, O. & LOBITZER, H. (2007): Early Norian Scleractinian Corals and Microfacies Data of the Dachstein Limestone of Feisterscharte, Southern Dachstein Plateau (Northern Calcareous Alps, Austria). – Jb. Geol. B.-A., **147**, 577–594, Wien.

SALAJ, J. & STRANIK, Z. (1970): Rhetien dans l'atlas Tunisien oriental. – Notes Service Géologique Tunisie, **32**, 37–44, Tunis.

SALAJ, J., BORZA, K. & SAMUEL, O. (1983): Triassic Foraminifers of the West Carpathians. – Geologicky ústav Dionyza Stúra, 213 p., Bratislava.

SALAJ, J., TRIFONOVA, E. & GHEORGHIAN, D. (1988): A biostratigraphic zonation based on benthic foraminifera in the Triassic deposits of the Carpatho-Balkans. – Revue de Paléobiologie, vol. Spéc. Benthos, **86**, 153–159, Genève.

SCHÄFER, P. & SENOWBARI-DARYAN, B. (1978): Die Häufigkeitsverteilung der Foraminiferen in drei oberrhätischen Riff-Komplexen der Nördlichen Kalkalpen (Salzburg, Österreich). (Beiträge zur Paläontologie und Mikrofacies obertriadischer Riffe im alpinmediterranen Raum). – Verh. Geol. B.-A., **2**, 73–96, Wien.

SENOWBARI-DARYAN, B., SCHÄFER, P. & ABATE, B. (1982): Obertriadische Riffe und Rifforganismen in Sizilien (Beiträge zur Paläontologie und Mikrofazies obertriadischer Riffe im alpin-mediterranen Raum, 27). – Facies, **6**, 165–184, Erlangen.

SENOWBARI-DARYAN, B., RASHIDI, K. & TORABI, H. (2010): Foraminifera and their associations of a possibly Rhaetian section of the Nayband Formation in central Iran, northeast of Esfahan. – Facies. doi: 10.1007/s10347-0-10-0221-5.

WURM, D. (1982): Microfacies, Paleontology and Palecology of the Dachstein Reef Limestones (Norian) of the Gosaukamm Range, Austria. – Facies, **6**, 203–296, Erlangen.

ZAMPARELLI, V., IANNACE, A. & RETTORI, R. (1995): Upper Triassic foraminifers (Ammodiscidae) from the Scifarello Formation, S. Donato Unit (northern Calabria, Italy). – Revue de Paléobiologie, **14**, 399–409, Genève.

ZANINETTI, L. (1976): Les Foraminiferes du Trias. – Rivista Italiana Paleontologia e Stratigraphia, **82**, 1–258, Milano.

ZANINETTI, L. & MARTINI, R. (1993): *Bispiranella* et *Orthotrinacria* (Foraminiferes, Trias), nouvelle description et regroupement dans la famille des Orthotrinariidae (Milioliporacea). – Bolletino della Societa Paleontologica Italiana, **32**, 385–392, Modena.